Scaling and Systems Considerations in Pulsed Inductive Thrusters

IEPC-2007-192

Kurt A. Polzin*

NASA-Marshall Space Flight Center, Huntsville, AL 35812

Performance scaling in pulsed inductive thrusters is discussed in the context of previous experimental studies and modeling results. Two processes, propellant ionization and acceleration, are interconnected where overall thruster performance and operation are concerned, but they are separated here to gain physical insight into each process and arrive at quantitative criteria that should be met to address or mitigate inherent inductive thruster difficulties. The effects of preionization in lowering the discharge energy requirements relative to a case where no preionization is employed, and in influencing the location of the initial current sheet, are described. The relevant performance scaling parameters for the acceleration stage are reviewed, emphasizing their physical importance and the numerical values required for efficient acceleration. The scaling parameters are then related to the design of the pulsed power train providing current to the acceleration stage. The impact of various choices in pulsed power train and circuit topology selection are reviewed, paying special attention to how these choices mitigate or exacerbate switching, lifetime, and power consumption issues.

I. Introduction

PULSED inductive plasma thrusters are spacecraft propulsion devices in which energy is stored in a capacitor and then discharged through an inductive coil. The device is electrodeless, inducing a current in a plasma located near the face of the coil. Propellant is accelerated and expelled at a high exhaust velocity ($\mathcal{O}\left(10 \text{ km/s}\right)$) by the Lorentz body force arising from the interaction of the plasma current and the induced magnetic field. The electrodeless nature of these thrusters eliminates the lifetime and contamination issues associated with electrode erosion in conventional pulsed plasma thrusters (PPTs). A wider variety of propellants (e.g. CO_2, H_2O) are available for use when compatibility with metallic electrodes is no longer an issue. Moreover, pulsed accelerators can maintain constant specific impulse (I_{sp}) and thrust efficiency (η_t) over a wide range of input power levels by adjusting the pulse rate to maintain a constant discharge energy per pulse.

There are many pulsed inductive plasma acceleration concepts in existence. However, in this paper we limit our discussion to planar pulsed inductive thrusters, where the inductive coil takes the shape of a flat spiral (as illustrated schematically in Fig. 1). Within this subset of thrusters are the Pulsed Inductive Thruster (PIT)[1] and the Faraday Accelerator with Radio-frequency Assisted Discharge (FARAD).[2] Each of these concepts is described in-turn below.

The current, state-of-the-art PIT design (the PIT MkV and above) employs a 1 m diameter coil comprised of a set of single-turn spirals that form a Marx-generator coil geometry. Essentially, two capacitors are connected in series by two half-turn spiral conductors, with each capacitor connected to the coil through its own switch (see Fig. 2A). This single-turn spiral configuration is repeated nine times at offsets of $40°$ in Fig. 2B to yield the full coil. Neutral gas (propellant) injected from a nozzle located at the downstream end of the device propagates down the sides of a conical structure and spreads over the face of the acceleration coil. Once the propellant completely covers the coil face the capacitors are discharged through the acceleration
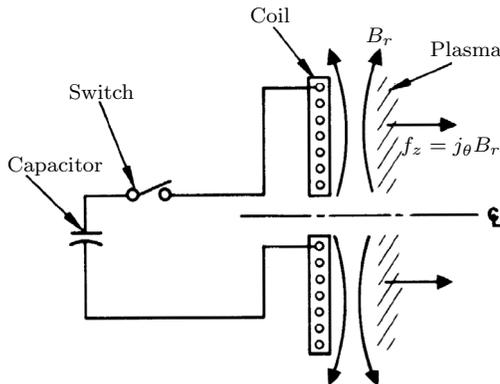
---

*Propulsion Research Engineer, Propulsion Research and Technology Applications Branch, Propulsion Systems Department. kurt.a.polzin@nasa.gov

coil to create a large azimuthal current, J_{Coil}. After a short but finite delay (ideally $< \mathcal{O}(10)$ ns), the current pulse ionizes the gas, forming a current sheet containing an induced current J_{Plasma}, which is subsequently accelerated by a $\mathbf{j} \times \mathbf{B}$ Lorentz body force.
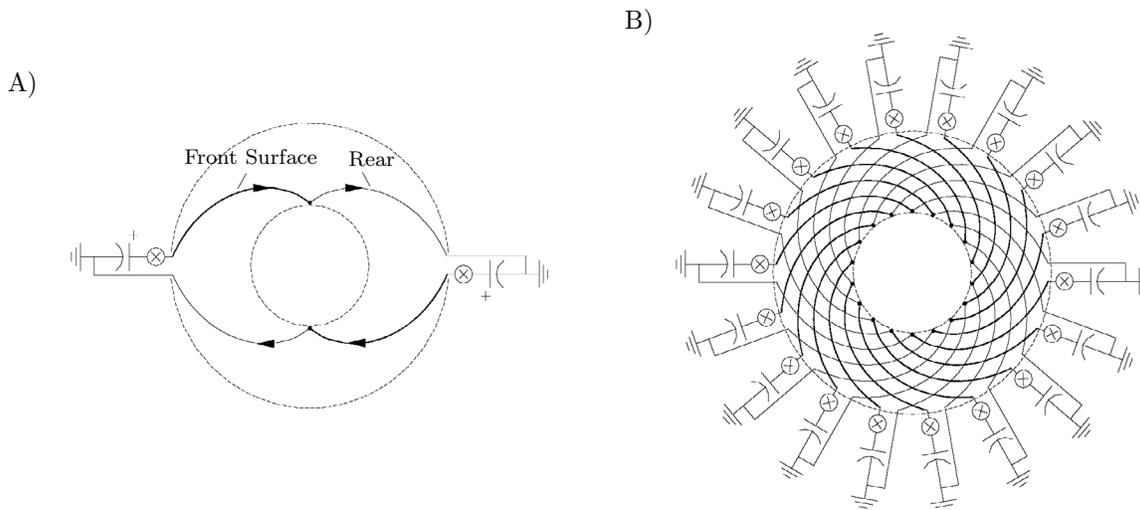
In FARAD, acceleration coils with diameters of 20 and 30 cm have been used. Neutral propellant is preionized by an inductive gas discharge (either pulsed or steady-state) as it expands over the face of the acceleration coil. Energy stored in the capacitor bank then discharges through the acceleration coil, coupling directly to the preionized gas, forming a current sheet, and giving rise to a Lorentz body force in the same manner as the PIT.

It is the purpose of this paper to explore the performance scaling of planar pulsed inductive thrusters over a broad range of sizes and operating parameters and to discuss the systems-level issues associated with the choice of the pulsed power train driving the acceleration. The results from PIT and FARAD experimental studies occupy very different parameter spaces. These differences, both in the operation and the operating regimes, are used to provide insight into the general performance scaling of pulsed inductive thruster operation.

Figure 1. Schematic showing the basic operation of a planar pulsed inductive plasma accelerator (after Ref. [3]).

The outline for the remainder of this paper is as follows. In Sect. II we state the major difficulties that confront the design of any pulsed inductive thruster. Scaling of the ionization process is discussed in greater detail in Sect. III, with acceleration scaling arguments and pulsed power train systems-level considerations following in Sect. IV. The results of this paper are briefly summarized in Sect. V.

Figure 2. Marx generator PIT coil configuration. A) One complete loop of a half-turn Marx generator. B) The nine complete loops comprising the PIT MkV. (from Ref. [4]).

II. Difficulties in Pulsed Inductive Thrusters

Two primary processes – ionization and acceleration – dominate the operation of pulsed inductive thrusters. Jahn has succinctly stated the following inherent difficulties pertaining to both ionization and acceleration that must be overcome in an efficient pulsed inductive accelerator:

"... inductive discharges embody two inherent electrodynamic disadvantages to conversion efficiency which detract from their propulsive effectiveness. First, any delay in breakdown of the gas after application of the primary field pulse results in energy being dissipated in the external circuit, which, unlike that of the direct electrode devices, is complete without the gas loop... This

difficulty might be relieved by providing a separate preionization mechanism or by operation at a sufficiently rapid repetition rate, but it is indicative of an inherent inefficiency in coupling of the external circuit to the plasma."

...

"Equally troublesome is the need to accomplish all the energy input to the gas before much motion of it has occurred. The current induced in the gasloop "secondary" depends on its mutual inductance with the external primary, and thus is a strong function of the physical separation of these two current paths. As they separate under the acceleration, the coupling rapidly becomes weaker."[5]

Put another way, if current is pulsed in the induction coil and there is no plasma, or the plasma is late in forming, the magnetic field produced by the coil (and the associated field energy) will radiate into space and be lost without performing any useful work. In addition, any acceleration of the plasma must occur very quickly before it gets too far from the acceleration coil and effectively decouples from the magnetic field induced by the current in the coil. In the next sections, we shall use experimental data from the literature and known performance scaling laws to justify quantitative criteria that should be met to address or mitigate the effects of these difficulties.

III. Ionization

Given the difficulties stated in the previous section, it is obvious that effective ionization of the propellant in a pulsed inductive thruster is a prerequisite for efficient acceleration. Energy cannot couple into the plasma if the plasma does not exist, so the time between when the current is pulsed in the acceleration coil and when the plasma is formed must be minimized. In addition, the ionization must be of a sufficient level to form a highly conductive, magnetically impermeable current sheet. If this does not occur, magnetic flux will resistively diffuse through the plasma and eventually escape into free space instead of performing work on the plasma. In this section, we subdivide data from PIT and FARAD experiments into two separate categories; those where a neutral propellant was acted on by the pulse of current through the acceleration coil, and those where the propellant was preionized before current was pulsed through the acceleration coil.

A. Without Preionization

The PIT has typically operated without preionization. That is, the current pulsing through the acceleration coil is responsible for both ionizing and accelerating the propellant. The results obtained for two early versions of this thruster (designated the PIT MkI and MkIV) were particularly insightful and discussed extensively in the literature.[6,7] In these experiments, $I_{\rm sp}$, $\eta_{\rm t}$, and the evolution of the magnetic field were measured for each thruster. The MkI coil was comprised of 24 single-turn spirals and had a 1 m diameter. The MkIV was a scaled down version of the MkI, possessing a coil diameter of 0.67 m. Both thrusters were operated using argon as a propellant. Performance of the MkI was significantly higher than the MkIV, with an $I_{\rm sp}$ of up to $\sim$2000 s and $\eta_{\rm t}$ of 30% as compared to $\sim$900 s and 15% in the MkIV. It was obvious from the magnetic field data that the field resistively diffused through the current sheet more rapidly in the MkIV, indicating lower conductivity in the plasma. Also, the MkIV showed additional current sheets forming after the first half cycle. This 'crowbarring' implies that the first current sheet did not effectively sweep the plasma out of the accelerated region, thus allowing for coupling between the external circuit and the remaining plasma during subsequent cycles. This was not observed in the MkI. It was concluded that the higher parasitic inductance found in the MkIV reduced the initial current rise rate, dI/dt, leading to an incomplete breakdown during the first half-cycle relative to the MkI.

The ionization process can be visualized with the help of Fig. 1. The current density in the coil is azimuthal, j_θ, and produces a magnetic field with components B_r and B_z in accordance with Ampere's law,

$$\nabla \times \mathbf{B} = \mu_0 \mathbf{j}.$$

Differentiating with respect to time demonstrates that the magnitude of the time-rate-of-change in the magnetic field scales linearly with the time-varying current density:

$$\frac{\partial |\mathbf{B}|}{\partial t} \sim \frac{\partial |\mathbf{j}|}{\partial t}.$$

A time-changing magnetic field induces an electric field in accordance with Faraday's law:

$$\nabla \times \mathbf{E} = -\frac{\partial \mathbf{B}}{\partial t}.$$

For the situation illustrated in Fig. 1, where the induced field in front of the coil is time-varying with the coil current density and has components B_r and B_z, we obtain an azimuthal electric field. At the beginning of a current pulse, the current density and magnetic field are increasing, so the induced electric field is in the direction opposite the current density:

$$E_\theta \sim -\frac{\partial j_\theta}{\partial t}.$$

Much like in a glow or arc discharge, it is the electric field that initially causes the gas to break down. In this case, it is the induced E_θ that controls the breakdown process and drives the plasma current. When current is first initiated in the coil, the rise rate scales like

$$\left.\frac{dI}{dt}\right|_{t=0} = \frac{V_0}{L_0},$$

where V_0 is the initial voltage on the capacitor and L_0 is the parasitic (non-coil) inductance. Considering the coil as a flat, two-dimensional plate with a length between the inner and outer radii equal to $\mathcal{L}$ and assuming that the current distribution is radially uniform over this face (see Fig. 3), we can write a scaling for the linear current density rise rate as

Figure 3. Schematic of a pulsed inductive accelerator coil face.

$$\left.\frac{dj_\theta}{dt}\right|_{t=0} = \frac{nV_0}{L_0\mathcal{L}},$$

where n represents the number of windings made by a single conductor in the coil. We conclude by relating the induced electric field to the coil and circuit parameters:

$$E_\theta|_{t=0} \sim -\frac{nV_0}{L_0\mathcal{L}}.$$

For a constant geometry coil, either increasing the charge voltage or decreasing the parasitic inductance in the circuit should lead to a greater induced electric field and, consequently, a shorter delay in the breakdown of the gas. We also expect that a decrease in the delay will result in an increase in the magnetic impermeability of the current sheet (i.e. reduced degree of magnetic diffusion through the sheet).

We can use the experimental data from the PIT MkI, MkIV, and MkV to place upper and lower bounds on the current density rise rate required to inductively produce a magnetically-impermeable current sheet from a propellant containing no preionization. Using argon as a propellant the performance of the MkI and MkV were comparable, implying that both were effective in ionizing the propellant. It is important to note that operating on ammonia propellant the MkV achieved better performance than the MkI; I_{sp} from 3000-8000 s and η_t of 45-50% for the MkV[1] compared to 1400-2200 s and 20-30% in the MkI.[8]

The estimated initial value of dj_θ/dt in the MkI[8] (based on $L_0 = 80$ nH, $V_0 = 22$ kV, $\mathcal{L} = 0.32$ m, and $n = 1$) is 860 kA/(m μs), while the value for the MkV[1] ($L_0 = 70$ nH, $V_0 = 30$ kV, $\mathcal{L} = 0.25$ m, and $n = 1$) is 1430 kA/(m μs). In both the MkI and MkV, internal plasma measurements and thruster performance indicated that the current sheet was well formed. However, in the MkIV internal measurements indicated a deficient current sheet. The value of L_0 in the MkIV is not accurately known, but direct experimental measurements[6] in both the MkI and MkIV show that the ratio $(E_\theta)_{\text{MkIV}}/(E_\theta)_{\text{MkI}}$ taken at $t = 0$ is roughly equal to 0.6, allowing us to estimate the initial value of $(dj_\theta/dt)_{\text{MkIV}}$ as 515 kA/(m μs). Using these values, we write a requirement on the current density rise rate in the case where the propellant is not preionized as:

$$515 \text{ kA/(m } \mu\text{s)} \;<\; \left.\frac{dj_\theta}{dt}\right|_{t=0} \;\leq\; 860 \text{ to } 1430 \text{ kA/(m } \mu\text{s)}.$$
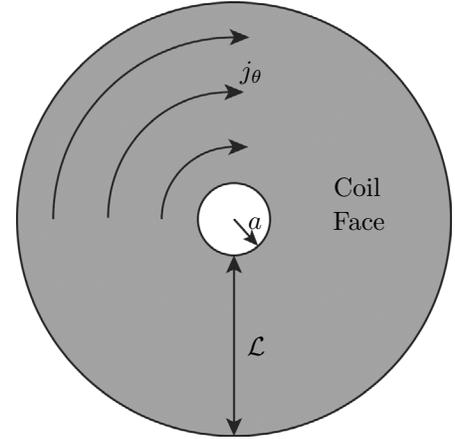
B. With Preionization

The purpose of preionization in a pulsed inductive thruster is to increase the conductivity of the propellant, making it easier for the second, main current pulse to completely break down the gas and induce a current sheet. The current sheet formation process is driven by the induced azimuthal electric field E_θ in the same manner as illustrated in the previous section. While preionization may not increase thruster efficiency at a given power level relative to the case with no preionization, we might expect a successful preionization scheme should help to lower the overall requirement on dj_θ/dt. One potential disadvantage of preionization is that it is only required in the region of the propellant where the current sheet is formed, so any preionization process that acts on the entire propellant distribution (bluk preionization) could represent an overall energy loss in the system.

Techniques used to preionize the gas on two smaller-scale PIT devices involved switching a lower-energy capacitor across an inductive coil, which served to partially break down the gas before the main pulse.[9, 10] In one of the thrusters, the preionization and main discharge pulses were both conducted through the same coil while in the other, a preionization pulse was conducted through a separate coil suspended in space 4 cm downstream from the primary acceleration coil. The coil geometry employed in the latter case resembled the acceleration coil.

In both preionization schemes, the initial pulse accomplished the goal of preionizing the propellant. However, in the case where the preionization pulse was passed through the acceleration coil, the plasma was also partially accelerated away from the coil face, reducing the electromagnetic coupling between the main discharge pulse and the plasma. This produced thruster performance that was significantly lower than the baseline case where no preionization was employed. In the case with the preionization coil located 4 cm downstream, a preionized current sheet was launched *towards* the acceleration coil. This served to compress the propellant and preionized gas into a thin, conductive region just above the acceleration coil and allowed for much greater coupling between the main coil current pulse and the plasma sheet. Consequently, the performance in this case was improved over the case where there was no preionization. In both cases, the preionization pulses through the coils managed to not only preionize the propellant but also to partially accelerate it, even though the preionization pulses were short in duration and low in energy relative to the main discharge pulse. Though it resulted in much improved performance, a preionization coil in the plume of the thruster was not retained as a design option because it would experience severe erosion due to ion bombardment over the duration of a mission.

In the FARAD, preionization is accomplished through the use of an inductive RF discharge in a process that is completely decoupled from the acceleration coil's operation. An inductive RF discharge forms a non-moving preionized plasma over the acceleration coil face. This contrasts with creating a plasma by flowing an electrical pulse of current through the acceleration coil, which as noted above both preionizes and partially accelerates the propellant. A steady-state variation of inductive RF preionization was employed on a proof-of-concept experiment,[2, 11] with an applied magnetic field serving to guide the preionized plasma over the coil face. Presently, a pulsed RF discharge is planned for implementation on a laboratory-model thruster.[12]

Data from the FARAD proof-of-concept experiments indicate large variations in the location, motion, thickness, and current density of the current sheet as the background (ambient fill) pressure or applied magnetic field were varied.[11] These variations occurred while maintaining constant RF input power and acceleration stage discharge energy. In some cases, a very sharp, narrow current sheet formed, while in others a more diffuse plasma seemed to result. While further investigation of the details is still required, the observations lead to the general conclusion that the density and distribution of the preionized gas had a significant effect on the composition and temporal history of the current sheet. In addition, while the point of lowest inductance is generally taken as the location where the gas will break down and form a current sheet in a pulsed accelerator, the data indicate that in the presence of an axially-distributed preionized plasma the current sheet *can* form further downstream. This observation is in-line with the discussion of the smaller-scale PIT devices that employed pulsed preionization. Finally, no current sheet formed in the FARAD experiments without a preionized plasma present.

The current density rise rate in the FARAD proof-of-concept experiment[2, 11] (based on $L_0 = 90$ nH, $V_0 = 2$ kV, $\mathcal{L} = 0.12$ m, and $n = 1$) was 185 kA/(m μs), which was not enough to allow for a magnetically-impermeable current sheet to form. However, we know that a rise rate like that found in the PIT (with no preionization) is capable of ionizing a neutral gas. Consequently, the target rise rate in a pulsed inductive

thruster employing preionization should fall between these bounds:

$$185 \text{ kA/(m } \mu\text{s)} \quad < \quad \left.\frac{dj_\theta}{dt}\right|_{t=0} \quad \leq \quad 860 \text{ to } 1430 \text{ kA/(m } \mu\text{s)}.$$

IV. Acceleration

There are several important issues that arise when designing the acceleration stage of an inductive thruster. One is optimization of the performance, which is affected by values chosen for various circuit components comprising the stage. Another is the actual type of circuit used to drive current through the inductive coil, and how that choice can affect the design at both the operational and systems level. These issues and the strategies that can be employed when addressing them are discussed in turn below.

A. Performance Optimization

Recently, an analysis was undertaken in which the governing equations for a pulsed inductive accelerator consisting of a set of coupled circuit equations and a one-dimensional momentum equation were nondimensionalized.[11, 13] This nondimensionalization led to the identification of several important dimensionless scaling parameters controlling the performance of inductive accelerators. In addition, a full numerical study of the solutions to the set of equations was insightful in extracting the effects other parameters had on thruster performance. The relevant scaling parameters which emerge from the system of equations and their physical importance were previously presented in Ref. [13] and are briefly reviewed below. Solutions of the governing equations were generated in that previous paper assuming that the coil was connected to a single capacitor in an RLC system.

1. Inductance Ratio: L^*

The pulsed inductive accelerator circuit possesses an external inductance L_0 and an acceleration coil inductance L_C. Over the course of a current pulse the circuit's inductance can increase from L_0 to $L_0 + L_C$ (i.e. $L_C = \Delta L$). It is well known that the efficiency of a pulsed electromagnetic accelerator cannot exceed the fractional change of inductance, $(L^*)^{-1} = \Delta L/L_0$, as this ratio is a measure of the fraction of energy that can be deposited into electromagnetic acceleration of the gas. Consequently, we expect the value of L^* to be much less than unity or $L_C \gg L_0$ in an efficient pulsed inductive accelerator.

2. Critical Resistance Ratios: ψ_1 and ψ_2

The critical resistance ratios are defined as

$$\psi_1 = R_e\sqrt{\frac{C}{L_0}}, \qquad \psi_2 = R_p\sqrt{\frac{C}{L_0}},$$

where C is the capacitance in the circuit and R_e and R_p are the resistance of the external circuit and the plasma, respectively. These parameters, or more specifically their average, $\Psi \equiv (\psi_1 + \psi_2)/2$ controls the nature of the current waveform in the acceleration coil. The waveform is overdamped if $\Psi > 1$, critically damped for Ψ of unity, and underdamped (ringing) for $\Psi < 1$. A prior study found[13] that for greater efficiency and exhaust velocity, the current should peak while the plasma is still close to the acceleration coil, implying that underdamped circuits are preferable.

3. Dynamic Impedance Parameter: α

The dynamic scaling parameter, α, is similar to that found in the pulsed plasma thruster (PPT) literature. This parameter is defined in terms of measureable quantities and can be written as the product of several important ratios

$$\alpha = \frac{C^2 V_0^2 L_C}{2 m_{\text{bit}} z_0^2} = \frac{1}{8\pi^2} \frac{C V_0^2/2}{m_{\text{bit}} v_z^2/2} L^* \left(\frac{2\pi\sqrt{L_0 C}}{L_0/\dot{L}}\right)^2$$

where m_{bit} is the propellant mass per pulse, z_0 is the characteristic electromagnetic coupling distance for the thruster, $\dot{L}$ is the dynamic impedance which is defined as $v_z L'$, and L' is the effective inductance per

unit length, equal to L_C/z_0. The ratio of the initial stored energy to the plasma kinetic energy is recognized as the inverse of thrust efficiency, which will always be greater than one. The final term is the ratio of the resonant period of the unloaded circuit, $2\pi\sqrt{L_0 C}$, to the time it takes for the plasma motion to increase the inductance of the circuit by L_0, which is equal to $L_0/\dot{L}$. The former is the time scale on which the external circuit naturally operates, while the latter is essentially the time scale on which the current sheet remains in the acceleration region before decoupling from the coil (residence time).

When the ratio of the circuit time scale to the residence time is small ($\ll 1$), the external circuit attempts to transfer its energy faster than the current sheet can accept it, leading to an inefficient acceleration process. On the other hand, when the ratio of the time scales is large ($\gg 1$), the sheet moves away from the acceleration coil quickly, exiting the acceleration region and decoupling before the external circuit can transfer the maximum amount of energy to the sheet. Between these two cases exists an optimum value of α (see Fig. 4) where the residence time scale of the current sheet is matched to the external circuit, allowing for optimum transfer of stored electrical energy into directed kinetic energy. Solutions to the coupled circuit and momentum equations governing pulsed inductive thruster operation show that the optimum value of α depends upon the mass loading and is between 1 and 3 for maximum efficiency.[13] An interesting note from that study is that the thruster's efficiency remains relatively constant over a broad range of α, a fact that was previously found experimentally[1] but never fully explained. The nondimensional parameters for different PIT MkV data are plotted as "+" symbols in Fig. 4 and the measured thrust efficiencies associated with these points compare quite favorably with the computed performance contours in the graph.
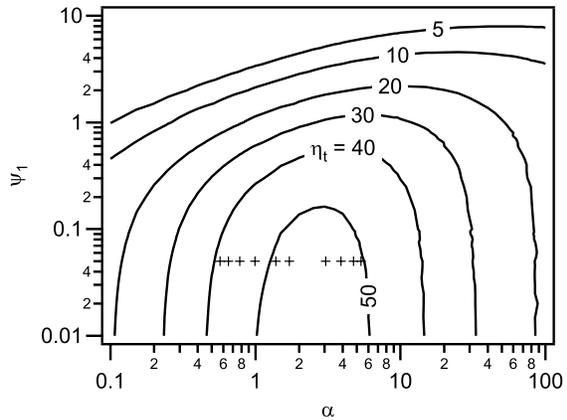
4. Propellant Distribution

The propellant distribution can have a profound effect on the efficiency of a pulsed inductive thruster. The performance improves as a greater fraction of the propellant is distributed near the acceleration coil, and is optimized with a slug mass propellant loading. This optimization is primarily due to the drag associated with a moving current sheet entraining and accelerating any propellant it encounters. An inductively driven current sheet propagating into propellant with substantial velocity experiences significant drag (drag force $\propto v_z^2$) while at the same time the driving force applied to the current sheet from the coil is decreasing exponentially with increasing axial position. As a consequence, the thrust efficiency can be as high as 70% for a slug mass loading, but drops to only 16% for a uniform density over the face of the coil.[13]

Figure 4. **Contour plots of inductive accelerator efficiency as a function of α and ψ_1 for a mass distribution like that found in the PIT MkV. Fixed nondimensional parameters in these computations are $\psi_2 = 0.13$, $L^* = 0.121$. Points corresponding to the nondimensional parameters found in the PIT MkV are indicated by "+" symbols.[1]**

B. Circuit Topology

There are two separate issues that must be taken into account when designing the circuit topology for a pulsed inductive thruster. The circuit must meet the electrical specifications (current rise times, lumped element circuit parameter values) dictated by the above-listed rules to both form a magnetically-impermeable current sheet and then accelerate it efficiently. However, there are also component and systems-level issues that also require attention. The switches in pulsed inductive thrusters must be capable of holding off $\mathcal{O}(1000\text{ V})$ while switching at least $\mathcal{O}(10\text{ kA})$ of current with a response time of $\mathcal{O}(10\text{ ns})$. Moreover, they must be extremely long-lived to last for the approximately 10^9-10^{10} pulses needed to deliver an appreciable total impulse to a spacecraft. We discuss below several different approaches to address these circuit design issues.

The PIT originally employed a single capacitor bank connected to the acceleration coil to form a simple RLC circuit. In models starting with the PIT MkV, a Marx-generator configuration like that shown in Fig. 2 was used. The Marx-generator geometry is a low inductance configuration at smaller coil sizes, so the PIT
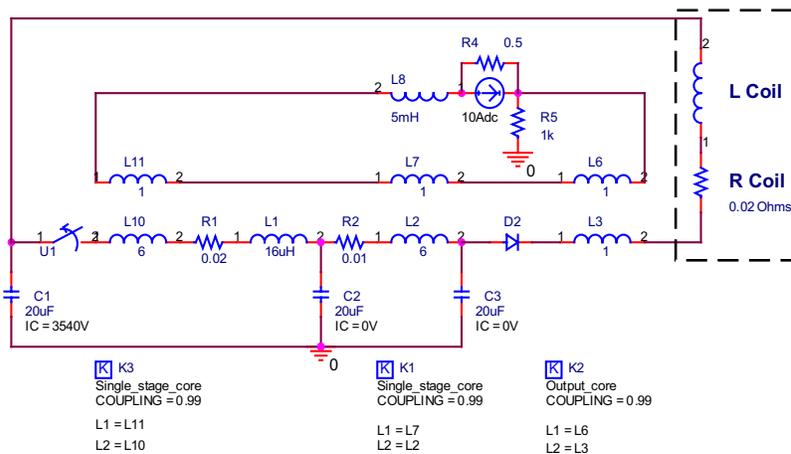
thruster dimension is large (1 meter) to yield a coil inductance great enough for effective electromagnetic acceleration. The response of these RLC systems is simple to model, and the topology of the PIT MkV allowed for low parasitic inductance *and* an initial charge voltage equal to twice the voltage applied to a single capacitor, significantly increasing the initial values of dI/dt in the circuit and dj_θ/dt in the coil. The discharge voltage and current rise rate requirements are high since the current pulse is required to first break down and then accelerate the gas. In both the single capacitor bank and Marx-generator configurations, solid-state components cannot presently meet the swtich requirements, spark-gap switches have been used instead. An additional difficulty is that the individual switches (either solid state or spark gap) on each capacitor in the Marx-generator must be triggered simultaneously for effective operation.

An alternative pulsed power train that may be employed is a pulse compressor, in which an initially slow, low-current pulse is compressed to yield a short, high-current pulse.[12, 15] The circuit depicted in Fig. 5 uses diode D2 to ensure that current can only flow through the coil in one direction, eliminating voltage reversal on the capacitors and helping to increase capacitor lifetime. Sample current and voltage waveforms for a single-stage pulse compressor are given in Fig. 6.

As previously alluded to, an issue that has been the subject of investigation in pulsed inductive thruster research and development is the implementation of solid-state switching. The problem is difficult in the general case where there is no propellant preionization since the switches must meet the voltage, current, and rise rate requirements for current-sheet formation without introducing additional stray inductance. A pulse compressor lends itself as an alternative circuit topology in which solid-state switching is possible using present switch technology since the pre-compressed current levels and rise rates are low enough to allow the use of solid-state components. A second way to circumvent this problem is to employ preionization, as it was used in the FARAD proof-of-concept experiment[2, 11] and in a low-energy FARAD thruster,[12] reducing the switching requirements and making the use of solid-state components possible.

Figure 5. PSPICE schematic model of a pulse compression ring circuit (from Ref. [12]).
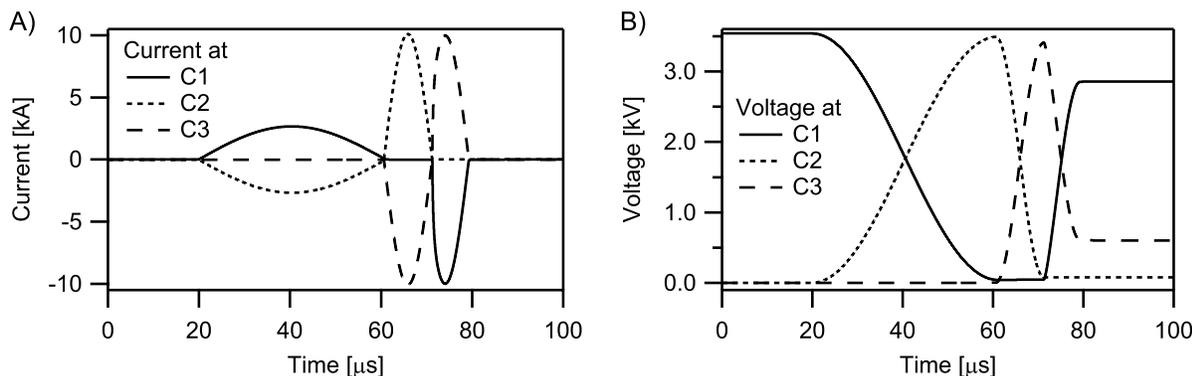
Figure 6. PSPICE simulation results giving A) current and B) voltage characteristics at each capacitor in a single-stage pulse compressor (from Ref. [12]).

A power train's ability to recapture unused energy and apply it to later pulses can help reduce the overall power system and radiator requirements, potentially making pulsed inductive thrusters more attractive for certain missions. The Bernardes and Merryman (B&M) circuit[14] is a pulsed power train designed to allow
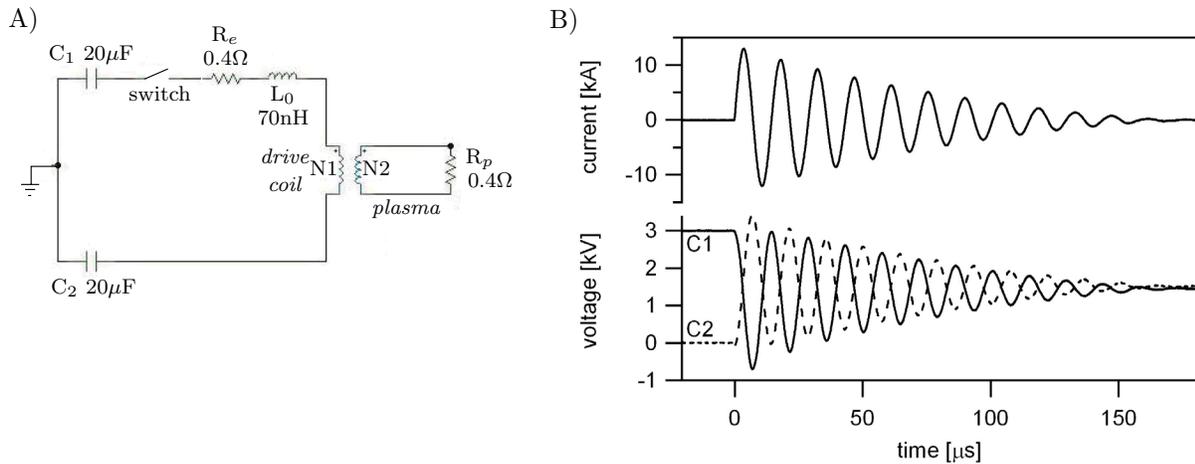
Figure 7. A) Typical B&M circuit schematic B) and current and voltage waveforms into a 540 nH inductive load for a 3 kV initial charge on capacitor C1. Voltages presented for both capacitors C1 and C2 (from Ref. [12]).
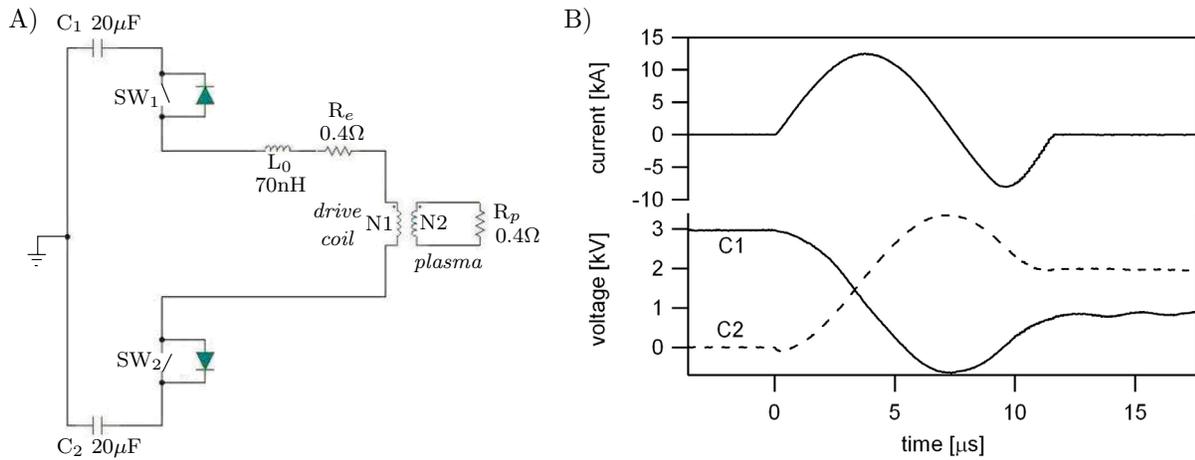

Figure 8. A) Typical diode-latched B&M circuit schematic B) and current and voltage waveforms for a 3 kV initial charge on capacitor C1. Voltages presented for both capacitors C1 and C2 (from Ref. [12]).

for energy recapture. The basic B&M circuit shown schematically in Fig. 7A is a variation on a simple RLC circuit, possessing two capacitor banks of equal capacitance. Sample waveforms showing the discharge current and capacitor voltages are presented in Fig. 7B. The data show that residual voltage remains on each capacitor after a pulse. This voltage represents energy that can, in part, be recovered and used for the next pulse. We observe that the topology also precludes voltage reversals on either capacitor, reducing the stress and increasing their operational lifetimes. (Note: the pulse compressor illustrated in Fig. 5 is a derivative of the B&M circuit topology.)

The B&M circuit's energy recovery potential may be further improved upon by employing a latching design.[12] A circuit schematic of this concept is shown in Fig. 8A, where latching diodes have been added in parallel to the two switches; one for each capacitor bank. The diodes serve to reduce the amount of energy resistively dissipated in the discharge by allowing current to flow in the circuit for only the first half-cycle of the discharge. The initially uncharged capacitor bank is partially charged by the current flowing through the coil from C_1 to C_2 (see Fig. 8B), reducing the amount of charge that must be applied to bank C_2 before the next pulse. This scheme effectively recaptures additional energy that would otherwise have been lost in a standard B&M circuit.

V. Conclusions

We have presented scaling arguments and parameters that explain and control the performance of pulsed inductive thrusters over a range of sizes and operating parameters. These parameters apply to the two distinct and inherent processes found in these thrusters: ionization and acceleration. The scaling arguments were based on analytical and numerical modeling and performance data from both the PIT and FARAD, which operate under very different conditions. The effect of azimuthal current density rise rate in the coil on plasma ionization and current sheet formation was shown, and experimental data was used to bound the rise rate in cases with and without the use of preionization. The relevant acceleration scaling parameters, their physical meanings, and their influence on the performance of pulsed inductive thrusters were discussed, and values were identified for high-efficiency operation. The systems-level impacts of various design choices, both for the ionization and acceleration processes, were described with a focus on how various pulsed power trains and circuit topologies can either mitigate or exacerbate certain design problems such as switching, lifetime, and power consumption.

Acknowledgments

References

[1] C.L. Dailey and R.H. Lovberg, *The PIT MkV Pulsed Inductive Thruster*, Tech. Rep. NASA CR-191155, TRW Systems Group, July 1993.

[2] E.Y. Choueiri and K.A. Polzin, "Faraday Acceleration with Radio-frequency Assisted Discharge," *J. Propuls. Power*, **22**(3):611, May-June 2006.

[3] R.H. Lovberg and C.L. Dailey, "Large inductive thruster performance measurement,", *AIAA J.*, **20**(7):971, July 1982.

[4] R.H. Lovberg and C.L. Dailey, *A PIT Primer*, Technical Report 005, RLD Associates, Encino, CA, 1994.

[5] R.G. Jahn, *Physics of Electric Propulsion*, McGraw-Hill, New York, 1968.

[6] C.L. Dailey and R.H. Lovberg, *PIT Clamped Discharge Evolution*, Tech. Rep. AFOSR-TR-89-0130, TRW Space and Technology Group, Redondo Beach, CA, Dec. 1988.

[7] R.H. Lovberg and C.L. Dailey, "Current sheet development in a pulsed inductive accelerator," 25th *AIAA/SAE/ASME/ ASEE Joint Propulsion Conference*, Monterey, CA, June 1989. AIAA Paper 89-2266.

[8] C.L. Dailey and R.H. Lovberg, *Pulsed Inductive Thruster Component Technology*, Tech. Rep. AFAL-TR-87-012, TRW Space and Technology Group, Redondo Beach, CA, April 1987.

[9] C.L. Dailey, *Pulsed electromagnetic thruster*, Tech. Rep. AFRPL-TR-71-107, TRW Systems Group, Redondo Beach, CA, Dec. 1971.

[10] C.L. Dailey and H.A. Davis, *Pulsed plasma propulsion technology*, Tech. Rep. AFRPL-TR-73-81, TRW Systems Group, Redondo Beach, CA, July 1973.

[11] K.A. Polzin, *Faraday Accelerator with Radio-frequency Assisted Discharge*, Ph.D. Dissertation, 3147-T, Princeton Univ., Princeton, NJ, 2006.

[12] K.A. Polzin, M.F. Rose, R. Miller, S. Best, T. Owens, and J. Dankanich, "Design of a Low-Energy FARAD Thruster," *43rd AIAA/ASME/SAE/ASEE Joint Propuls. Conf.*, Cincinnati, OH, July 2007. AIAA Paper 2007-5257.

[13] K.A. Polzin and E.Y. Choueiri, "Performance Optimization Criteria for Pulsed Inductive Plasma Acceleration," *IEEE Trans. Plasma Sci.*, **34**(3):945, June 2006.

[14] J. Bernardes and S. Merryman, "Parameter Analysis of a Single Stage Induction Mass Driver," *Proc. 5th IEEE Int'l Pulsed Power Conf.*, M.F. Rose and P.J. Turchi, ed., pp. 552-555, Arlington, VA, 1985. Paper PI-27.

[15] D.L. Birx, P.P. Das, I.V. Fomenkov, W.N. Partlo, and T.A. Watson, "Pulse power generating circuit with energy recovery," U.S. Patent 5,729,562, 1998.